J. Fluid Mech. (2001), *vol.* 439, *pp.* 353–366. Printed in the United Kingdom

An integral model for gas entrainment into full cone sprays

By G. E. COSSALI

Facoltà di Ingegneria, Università di Bergamo, Via Marconi, 6, I-24044 Dalmine (BG), Italy

(Received 17 May 2000 and in revised form 22 January 2001)

The paper proposes a one-dimensional model for predicting gas entrainment into a non-evaporating full cone steady spray injected into a stagnant gas at uniform pressure. The main outcome is a law relating the entrained mass flow rate to injected mass flow rate, gas properties, mean droplet diameter and axial distance from the nozzle. A comparison with available experimental data is presented. The model allows the apparent inconsistency of the experimental results obtained under different conditions to be eliminated by identifying two new non-dimensional parameters.

1. Introduction

The fluid mechanics of a spray is controlled by a multitude of phenomena, like atomization, turbulence generation, droplet interaction with a turbulent flow, droplet instability and break-up, coalescence, drop–gas heat and mass exchange, etc., most of which are still not fully understood. The usual way to tackle such a challenging problem is by means of numerical solution of a set of integral-differential equations which are expected to describe all the phenomena mentioned above, and many attempts can be found in the literature (O'Rourke & Bracco 1980; Reitz & Diwakar 1982; Watkins, Gosman & Tabrizi 1986; Reitz 1987).

One of the most evident macroscopic effects of injecting a pressurized liquid into a gaseous atmosphere through a narrow passage, under conditions able to produce the complete atomization of the liquid, is the gas entrainment into the spray cone, a phenomenon produced by the momentum exchange between the injected and the ambient fluid. While gas entrainment into a steady turbulent gaseous jet injected into quiescent atmosphere has been extensively studied both theoretically (Schlichting 1968) and experimentally (Ricou & Spalding 1961; Hill 1972), only recently has attention been devoted to gas entrainment into full cone liquid sprays, mainly because of its relevance in some applied fields, like IC engines where fuel combustion efficiency strongly depends on the fuel–air mixing.

For steady gaseous jets, a linear dependence of the entrained mass flow rate on the distance from the nozzle is observed and a proper definition of the entrainment coefficient, independent of the distance from nozzle, injection conditions and gas properties (as long as the jet Reynolds number is sufficiently high (Schlichting 1968)), can be given. In full cone steady sprays such a definition was proven to be inadequate (Ruff, Sagar & Faeth 1988), producing an entrainment coefficient depending on the distance from the nozzle, and also the use of another definition of the entrainment coefficient (or non-dimensional entrainment rate) has given inconsistent results when applied to steady (Ruff *et al.* 1988; Hosoya & Obokata 1992) and unsteady (Cossali, Brunello & Coghe 1991) sprays.

The present work is intended to provide a model for predicting entrainment into full cone non-evaporating steady sprays and to give a consistent explanation of the experimental findings. The next section is devoted to the development of the proposed model, then, in § 3, limiting solutions of the entrainment equation are derived and compared, in § 4, to existing experimental data. In § 5 the effect of the approximations introduced during the model development is addressed and § 6 summarizes the conclusions.

2. The mass and momentum conservation equations

Let us consider a steady spray injected through a circular orifice drilled in a plate extending to infinity in two dimensions and separating the injected fluid from the quiescent atmosphere. The origin of the axial coordinate z is taken at a location positioned upstream or downstream of the nozzle, so that the nozzle position in such a coordinate system is z_o. Cylindrical symmetry is assumed and buoyancy effects are neglected. Incompressibility of liquid and gaseous phases is assumed. Writing the model equations other simplifying hypothesis are introduced whose validity, limitations and implications will be discussed in a subsequent section. In a non-evaporating spray, mass and momentum balances can be written separately for the liquid and gaseous phases.

2.1. *The gas phase*

The gas mass flow rate crossing a plane normal to the z-axis and positioned at a distance z from the origin is

$$\dot{m}_e(z) = \int_0^\infty \rho_g v(z,r) 2\pi r \, \mathrm{d}r, \tag{1}$$

where $v(z,r)$ is the mean axial velocity at the location (z,r). The axial gas momentum flux through the same plane is

$$J^g(z) = \int_0^\infty \rho_g v^2(z,r) 2\pi r \, \mathrm{d}r, \tag{2}$$

where turbulence has been neglected. Taking into account the turbulence in the gas phase should be written as

$$J^g(z) = [1 + C_t(z)] \int_0^\infty \rho_g v^2(z,r) 2\pi r \, \mathrm{d}r, \tag{3}$$

with

$$C_t(z) = \frac{\displaystyle\int_0^\infty \rho_g \overline{v'^2}(z,r) r \, \mathrm{d}r}{\displaystyle\int_0^\infty \rho_g v^2(z,r) r \, \mathrm{d}r},$$

and $\overline{v'^2}(z,r)$ is the turbulence fluctuation along the axial direction. Values of $C_t(z)$ are not available for the present flow. For a turbulent gaseous round jet a numerical integration of the data from Wygnanski & Fiedler (1969) gives $C_t \approx 0.2$ (independent of z if $z/D > 50$). Although this value cannot be considered negligible, the effect of accounting for it would be to introduce an unknown multiplying constant (if self-similarity of turbulence intensity holds) in equation (2), which could be easily included into one of the constants appearing in the model (for example in M, equation (9)). This observation partially justifies the above-mentioned approximation.

The integral balance of the axial gas momentum component in a portion of space between two planes normal to the spray axis and located at distances z_1 and z_2 from the origin ($z_2 > z_1$) can be written as

$$J^g(z_2) - J^g(z_1) = J_s^g(z_1, z_2), \tag{4}$$

where $J_s^g(z_1, z_2)$ is the total momentum source between the planes at z_1 and z_2 produced by the momentum transfer from the liquid drops to the ambient gas.

In the following the mean axial gas velocity profiles will be considered self-similar, i.e.

$$v(r, z) = W(z)\, f(r/z). \tag{5}$$

It is expected that such an assumption will not hold very close to the nozzle and in § 5 the effect of this approximation will be discussed.

On using equation (5) the entrained mass flow rate and the gas momentum flux become

$$\dot{m}_e(z) = \int_0^\infty \rho_g v(z, r) 2\pi r \, \mathrm{d}r = 2\pi W(z) z^2 \rho_g Q, \tag{6}$$

$$J^g(z) = \int_0^\infty \rho_g v^2(z, r) 2\pi r \, \mathrm{d}r = 2\pi \; W^2(z) \; z^2 \rho_g M, \tag{7}$$

with

$$Q = \int_0^\infty f(\xi) \xi \, \mathrm{d}\xi, \tag{8}$$

$$M = \int_0^\infty f(\xi)^2 \xi \, \mathrm{d}\xi; \tag{9}$$

$\xi = r/z$ and $f(0) = 1$.

The boundary condition $v(r, z_o) = 0$, due to the solid wall at $z = z_o$, and equation (4) give

$$J_s^g(z_o, z) = J^g(z) = 2\pi W^2(z) z^2 \rho_g M = \frac{\dot{m}_e^2(z) M}{2\pi z^2 \rho_g Q^2}, \tag{10}$$

the last equality coming from equation (6).

2.2. *The liquid phase*

The injected mass flow rate is related to the average liquid velocity u_o at the nozzle exit by

$$\dot{m}_o = \int_0^R \rho_o u_l(0, r) 2\pi r \, \mathrm{d}r = \rho_o u_o \frac{D^2 \pi}{4}, \tag{11}$$

where $u_l(0, r)$ is the liquid axial velocity distribution at the nozzle exit, ρ_o is the liquid density and $D = 2R$ the nozzle diameter. The liquid momentum flux through the nozzle is then:

$$J_o = \int_0^R \rho_o u_l^2(0, r) 2\pi r \, \mathrm{d}r = C_M \dot{m}_o u_o = C_M \frac{\dot{m}_o^2 4}{D^2 \pi \rho_o}, \tag{12}$$

where

$$C_M = \frac{R^2 \displaystyle\int_0^R u_l^2(0, r) r \, \mathrm{d}r}{2 \left(\displaystyle\int_0^R u_l(0, r) r \, \mathrm{d}r \right)^2} \leqslant 1$$

is the factor that accounts for a non-uniform exit velocity profile (the equality holds for a uniform velocity profile).

To write the mass and momentum conservation equation for the liquid phase, self-similarity of the drop velocity and drop number concentration profiles will be assumed:

$$u(r,z) = U(z)\theta(\xi), \quad n(r,z) = N(z)\varphi(\xi), \tag{13}$$

where $u(r,z)$ is the mean axial drop velocity and $n(r,z)$ the mean drop number concentration and $\theta(0) = \varphi(0) = 1$. Again this approximation may not hold very close to the nozzle; however there exists evidence (Wu *et al.* 1984) that self-similarity of drop velocity is approached downstream of the nozzle.

The liquid-phase mass flow rate through a plane normal to the z-axis at location z is then

$$\begin{aligned}\dot{m}_l(z) &= \int_0^\infty n(r,z)u(r,z)\tfrac{1}{6}\rho_o\pi d^3(z)2\pi r\,\mathrm{d}r \\ &= N(z)U(z)2\pi z^2 B\tfrac{1}{6}\rho_o\pi d^3(z) = \dot{m}_o,\end{aligned} \tag{14}$$

with

$$B = \int_0^\infty \theta(\xi)\varphi(\xi)\xi\,\mathrm{d}\xi; \tag{15}$$

$d(z)$ is an average drop diameter over the plane at z (equation (14) can be considered a definition of $d(z)$) and the last equality comes from mass conservation of the liquid phase, which excludes evaporation.

The liquid-phase axial momentum flux through the plane at z can be evaluated as

$$\begin{aligned}J^l(z) &= \int_0^\infty n(r,z)u^2(r,z)\tfrac{1}{6}d'^3(z)\pi\rho_o 2\pi r\,\mathrm{d}r \\ &= N(z)U^2(z)2\pi z^2\tfrac{1}{6}d'^3(z)\pi\rho_o C,\end{aligned} \tag{16}$$

where

$$C = \int_0^\infty \theta^2(\xi)\varphi(\xi)\xi\,\mathrm{d}\xi \tag{17}$$

and $d'(z)$ may be different from $d(z)$ (again equation (16) can be considered a definition of $d'(z)$).

The liquid-phase momentum balance for the portion of space between z_o and z can be written as

$$J^l(z) - J^l(z_o) = J_s^l(z_o,z) = -J_s^g(z_o,z), \tag{18}$$

where $J_s^l(z_o,z)$ is the momentum source (or sink) into the liquid phase and the last equality comes from the total momentum conservation. $J^l(z_o)$ can be promptly evaluated as $J^l(z_o) = J_o$.

The momentum sink $J_s^l(z_o,z)$ can be estimated as the total drag force acting on all the drops contained between the planes at z_o and z. The aerodynamic drag on a sphere moving through a gaseous medium can be evaluated by the relation (see Lee & Reitz 1999)

$$f_D = 3\pi\mu d''(v_g - u_d)(1 + \tfrac{1}{6}Re^{2/3}), \tag{19}$$

where $Re = (|v_g - u_d|\rho_g d'')/\mu$, μ is the gas viscosity, v_g and u_d are the gas and drop

velocity and d'' is the drop diameter. The momentum sink $J_s^l(z_o, z)$ is then

$$J_s^l(z_o,z) = \int_{z_o}^{z}\int_0^{\infty} n(r,z) f_D 2\pi r \,\mathrm{d}r\,\mathrm{d}z$$
$$= \int_{z_o}^{z}\int_0^{\infty} N(z) 3\pi\mu d''(z) 2\pi z^2 U(z) \left(\frac{W(z)}{U(z)} f(\xi) - \theta(\xi)\right)$$
$$\times \left\{1 + \frac{1}{6}\left(\frac{\rho_g d''(z) U(z)}{\mu}\right)^{2/3} \left|\frac{W(z) f(\xi)}{U(z)} - \theta(\xi)\right|^{2/3}\right\} \varphi(\xi)\xi \,\mathrm{d}\xi\,\mathrm{d}z. \quad (20)$$

The three drop diameters $d(z)$, $d'(z)$, $d''(z)$ introduced here are, in principle, different as they represent averages of drop diameters over the plane located at z, evaluated taking different weight functions (as it can be appreciated comparing equations (14), (16) and (20)). There may exist relations among them that however will depend on the actual drop size and velocity distribution.

2.3. *The entrainment equation*

It is now convenient to introduce the non-dimensional quantity $\Lambda(z) = \dot{m}_e(z) D/(\dot{m}_o z)$, then equation (10) can be re-written using equation (12) giving

$$\Lambda(z) = \frac{\dot{m}_e(z) D}{\dot{m}_o z} = \left(\frac{8Q^2 C_M}{M}\right)^{1/2} \left(\frac{\rho_g}{\rho_o}\right)^{1/2} \left(\frac{J_s^g(z_o,z)}{J_o}\right)^{1/2}. \quad (21)$$

Equation (21) gives the relation between entrainment and momentum exchange between liquid and gaseous phases and shows that a linear dependence of the entrained mass flow rate on z is found only when $J_s^g(z_o, z)$ is constant.

The model allows a compact solution if the following assumption is added:

$$\theta(\xi) = f(\xi), \quad (22)$$

i.e. the gas velocity distribution is similar to the drop velocity distribution (although the magnitude is obviously different). Such a condition is verified when drop and gas are in equilibrium, but no experimental evidence exists for the validity of equation (22). The effects of this assumption will be discussed in § 5.

Using equations (14) and (22), equation (20) becomes

$$J_s^l(z_o,z) = \frac{18\dot{m}_o\mu}{\rho_o} \int_{z_o}^{z} \frac{d''(z)}{d(z)^3} \left(\frac{W(z)}{U(z)} - 1\right)$$
$$\times \left\{1 + \frac{1}{6}\left(\frac{\rho_g d''(z) U(z)}{\mu}\right)^{2/3} \left|\frac{W(z)}{U(z)} - 1\right|^{2/3} \frac{R}{B}\right\} \mathrm{d}z, \quad (23)$$

with

$$R = \int_0^{\infty} f(\xi)|f(\xi)|^{2/3} \varphi(\xi)\xi \,\mathrm{d}\xi. \quad (24)$$

From equations (10), (18) and (21)

$$J_s^l(z_o,z) = -\Lambda^2(z) \frac{\dot{m}_o^2 M}{D^2 2\pi\rho_g Q^2}; \quad (25)$$

then, combining equations (23) and (25) and taking the derivative gives

$$\frac{\mathrm{d}\Lambda^2(z)}{\mathrm{d}z} = -\frac{18\mu D^2}{\dot{m}_o}\frac{\rho_g}{\rho_o}\frac{2\pi Q^2}{M}\frac{d''(z)}{d(z)^3}\left(\frac{W(z)}{U(z)}-1\right) \times\left\{1+\frac{1}{6}\left(\frac{\rho_g d''(z)U(z)}{\mu}\right)^{2/3}\left|\frac{W(z)}{U(z)}-1\right|^{2/3}\frac{R}{B}\right\}. \tag{26}$$

The following notation will be used: $\zeta = z/D$, and for indicating a function of z and the corresponding function of ζ the same symbol will be used (i.e. $f(\zeta D) \equiv f(z) \equiv f(\zeta)$). After introduction of the function

$$G(\zeta) = \frac{QC}{MB}\left(\frac{d'(\zeta)}{d(\zeta)}\right)^3\frac{\Lambda(\zeta)}{\zeta(F-\Lambda(\zeta)^2)} - 1 = \frac{W(\zeta)}{U(\zeta)} - 1 \tag{27}$$

and few manipulations (see the Appendix for details) equation (26) becomes

$$\frac{\mathrm{d}\Lambda^2(\zeta)}{\mathrm{d}\zeta} = -18\left(\frac{\mu D}{\dot{m}_o}\right)\left(\frac{\rho_g}{\rho_o}\right)\left(\frac{2\pi Q^2}{M}\right)\left(\frac{D^2 d''(\zeta)}{d(\zeta)^3}\right)G(\zeta) \times\left\{1+\frac{1}{6}\left[\frac{BM}{2\pi CQ^2}(F-\Lambda(\zeta)^2)\frac{d''(\zeta)}{D}\left(\frac{d(\zeta)}{d'(\zeta)}\right)^3\frac{\dot{m}_o}{\mu D}\right]^{2/3}\frac{R}{B}|G(\zeta)|^{2/3}\right\}, \tag{28}$$

with

$$F = \frac{\rho_g}{\rho_o}\frac{8Q^2 C_M}{M},$$

and the boundary condition becomes

$$\Lambda(\zeta_o) = 0, \tag{29}$$

with $\zeta_o = z_o/D$.

3. Limiting solutions

Equation (28) can be re-written in a more compact form under the condition that the drop diameters d, d', d'' can be considered independent of the axial coordinate. By introducing the following variables and parameters:

$$\Phi = \frac{\Lambda}{\sqrt{F}}, \quad \eta = \frac{\alpha}{F}\zeta,$$

$$\alpha = \left(\frac{\mu D}{\dot{m}_o}\right)\left(\frac{\rho_g}{\rho_o}\right)\left(\frac{36\pi Q^2}{M}\right)\left(\frac{D^2 d''}{d^3}\right),$$

$$\varepsilon = \left(\frac{\rho_g}{\rho_o}\right)^{-1/2}\left(\frac{\mu D}{\dot{m}_o}\right)\left(\frac{D^2 d'^3 d''}{d^6}\right)\left(\frac{9\pi}{4\sqrt{2}}\frac{C}{M^{1/2}BC_M^{3/2}}\right),$$

$$\sigma = \left(\frac{\rho_g}{\rho_o}\right)^{2/3}\left(\frac{\mu D}{\dot{m}_o}\right)^{-2/3}\left(\frac{d''d^3}{Dd'^3}\right)^{2/3}\left(\frac{2}{\pi^2 27}\frac{R^3 C_M^2}{BC^2}\right)^{1/3},$$

the function $G(\zeta)$ becomes

$$G = G(\Phi, \varepsilon) = \frac{\varepsilon\Phi/\eta - (1-\Phi^2)}{(1-\Phi^2)},$$

equation (28) becomes

$$\frac{\mathrm{d}\Phi^2}{\mathrm{d}\eta} = -G(\Phi,\varepsilon)[1+\sigma|G(\Phi,\varepsilon)(1-\Phi^2)|^{2/3}], \tag{30}$$

and the boundary conditions are $\Phi(\eta_o)=0$ (where $\eta_o=\zeta_o\alpha/F$). The solution of the differential equation has then the form

$$\Phi = \Phi(\eta;\varepsilon,\sigma,\eta_o).$$

A first limiting solution of equation (30) can be found for $\eta\to\infty$: in this case the drop and gas velocities should become equal and $\lim_{\eta\to\infty} G(\eta)=0$. Equation (30) becomes

$$\frac{\mathrm{d}\Phi^2(\eta)}{\mathrm{d}\eta}=0$$

and the solution is $\Phi(\eta)=\text{const}$. From the condition $\lim_{\zeta\to\infty} U(\zeta)=0$ the constant is equal to 1 (see Appendix, equation (A 3)) so that

$$\frac{\dot m_e(z)}{\dot m_o}=\sqrt{F}\frac{z}{D}=\left(\frac{8Q^2C_M}{M}\right)^{1/2}\left(\frac{\rho_g}{\rho_o}\right)^{1/2}\frac{z}{D},$$

exactly as in gaseous jets, as should be expected considering that for large values of z the liquid-phase concentration becomes vanishingly small.

Another limiting solution can be found for $\eta\to\eta_o$ as the boundary condition (29) ensures that $\lim_{\zeta\to\zeta_o} G(\zeta)=\lim_{\eta\to\eta_o} G(\Phi(\eta),\varepsilon))=-1$. Equation (30) becomes

$$\frac{\mathrm{d}\Phi^2}{\mathrm{d}\eta}=[1+\sigma|(1-\Phi^2)|^{2/3}] \tag{31}$$

and a solution can be found in implicit form as

$$-(\eta-\eta_o)=\frac{3}{\sigma}\left\{(1-\Phi^2(\eta))^{1/3}-\frac{1}{\sqrt{\sigma}}\arctan\left[\sqrt{\sigma}(1-\Phi^2(\eta))^{1/3}\right]-C_o\right\}, \tag{32}$$

where $C_o=1-(1/\sqrt{\sigma})\arctan(\sqrt{\sigma})$. A first term truncation of the Taylor series expansion around $\Phi=0$ (i.e. $\eta=\eta_o$) gives the following explicit form:

$$\Phi(\eta)\simeq(\sigma+1)^{1/2}(\eta-\eta_o)^{1/2} \tag{33}$$

for $\Phi^2\ll 3(\sigma+1)/\sigma$, i.e. $\eta-\eta_o\ll 3/\sigma$ or $\zeta-\zeta_o\ll 3F/(\alpha\sigma)$.

It is interesting to notice that by setting $\gamma=\alpha^{1/2}(\sigma+1)^{1/2}$, and after introduction of the non-dimensional nozzle distance $y=(\zeta-\zeta_o)$, the ratio $\Psi=\dot m_e/(\sqrt{y}\dot m_o)$ will depend linearly on y:

$$\Psi=\frac{\dot m_e}{\sqrt{y}\dot m_o}=\gamma(y+\zeta_o). \tag{34}$$

Moreover, if σ is much larger than 1 equation (33) can be re-written as

$$\Lambda(\varsigma)\simeq H_o\left(\frac{\mu D}{\dot m_o}\right)^{1/6}\left(\frac{\rho_g}{\rho_o}\right)^{5/6}\left(\frac{D}{\bar d}\right)^{2/3}(\zeta-\zeta_o)^{1/2}, \tag{35}$$

with

$$H_o=\sqrt{3}\left(\frac{4}{\pi}\right)^{1/3}\left(\frac{2\pi Q^2RC_M^{2/3}}{MB^{1/3}C^{2/3}}\right)^{1/2},$$

and the mean diameter $\bar d=(d'^2d/d''^{5/3})^{3/4}$ has been introduced.

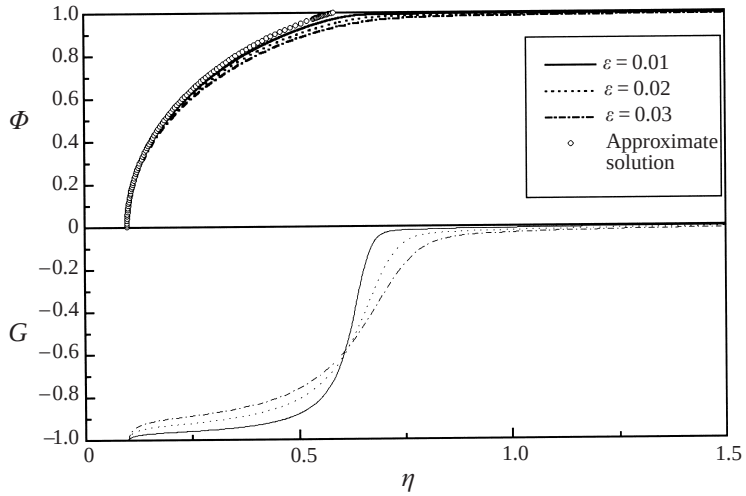

FIGURE 1. Numerical solution (curves) and limiting solution (32) (open symbols) of equation (30) for $\sigma = 2$, $\eta_o = 0.1$ and different values of ε. The parameters σ and ε depend on the non-dimensional parameters $\mu D/\dot{m}_o$ and ρ_g/ρ_o as reported in the text, while η is a corrected non-dimensional nozzle distance.

Equation (30) can be solved numerically and examples of solutions for $\eta_o = 0.1$, $\sigma = 2$ and different values of ε are reported in figure 1, together with the limiting solution (32), showing that this equation may represent correctly the actual solution, at least for values of ε not too large. To better appreciate the meaning of the curves reported in figure 1 it should be observed that from equation (21) and the definition of Φ

$$J_s^g(z_o, z) = J_o \Phi^2(z);$$

thus in the region where Φ differs considerably from 1 the drops are still transferring momentum to the gas, being decelerated by the drag. This is the region where the behaviour of a full cone spray differs considerably from that of a gas jet. Again from equation (21) and the definition of Φ

$$\Phi = \frac{m_e}{m_o(\rho_g/\rho_o)^{1/2}(8Q^2C_M/M)^{1/2}z/D}$$

showing that Φ may also be interpreted as the ratio between the actual entrained mass flow rate and that found in a gas jet of equal injected momentum and mass flow (see also the limiting solution for $\eta \to \infty$).

4. Comparison with experiments

Detailed quantitative data on gas entrainment into full cone steady sprays can be found only in few published works. To the knowledge of the author only Ha *et al.* (1984), Ruff *et al.* (1988), Hosoya & Obokata (1992) and Cossali *et al.* (1996) present complete quantitative data in a form that can be used to test the present model predictions. Ha *et al.* (1984) measured the ambient gas velocity magnitude around the spray cone by an I-type hot wire whereas flow direction was detected by smoke tracer. Ruff *et al.* (1988) reported LDV measurements of the surrounding gas from which entrainment was calculated. Hosoya & Obokata (1992) obtained the

Exp. no.	D (mm)	m_o (kg s^{-1}) ($\times 10^{-3}$)	μ_g (kg ms^{-1}) ($\times 10^{-5}$)	ρ_g/ρ_o ($\times 10^{-3}$)	$\mu_g D/\dot{m}_o$ ($\times 10^{-5}$)	γ ($\times 10^{-4}$)	ζ_o	$H_o(D/d)^{2/3}$
1	0.32	11.9	1.46	19.96	3.93	19.9	33.6	0.61
2	0.32	7.78	1.6	1.45	6.58	1.53	49.0	0.38
3	0.32	5.47	1.6	1.45	9.36	0.80	175.4	0.19
4	9.5	3990	1.6	1.18	0.381	0.64	6.6	0.30
5	19.1	11000	1.6	1.18	0.278	0.77	5.6	0.39
6	0.25	7.3	1.6	6.17	5.48	5.1	30.2	0.39
7	0.25	7.3	1.6	8.55	5.48	6.5	23.7	0.38
8	0.25	7.3	1.6	1.43	5.48	1.5	50.0	0.39

TABLE 1. Experiment parameters and values of the constants appearing in (34) and (35) for all the experiments: 1: Ha *et al.* (1984); 2 and 3: Hosoya & Obokata (1992), 4 and 5: Ruff *et al.* (1988); 6, 7 and 8: Cossali *et al.* (1996).

entrained mass flow rate from direct LDV measurement of the gas velocity. Cossali *et al.* (1996) measured by LDV the velocity of the gas entering an ideal cylindrical surface surrounding the spray cone, from which the entrained mass flow rate was calculated. Table 1 shows the main characteristics of these experiments.

The values of some parameters were not published and they were evaluated from the information given in the papers, e.g. to evaluate $\dot{m}_o$ (when not reported) the following formula was used:

$$\dot{m}_o = C_D \sqrt{2(P_{inj} - P_{gas})\rho_o} \frac{D^2\pi}{4}, \tag{36}$$

where C_D is the nozzle discharge coefficient which was evaluated to be about 0.8 for Hosoya & Obokata's (1992) and Ruff *et al.*'s (1988) experiments, and the same value was used for Ha *et al.*'s (1984) experiment; ambient gas density and viscosity were evaluated at standard atmospheric conditions when not otherwise stated. For diesel oil density, nominal values were assumed, but it must be recalled that this property may vary in a fairly wide range for different diesel oils, which are blends of different hydrocarbons.

For experiments 4 to 8 the results were reported in the form of normalized entrainment rate defined by the equation

$$K_e = \frac{\mathrm{d}\dot{m}_e}{\mathrm{d}z} \frac{D}{\dot{m}_o} \left(\frac{\rho_o}{\rho_g}\right)^{1/2},$$

and the entrained mass flow rate was obtained by integration. For experiment 1 (Ha *et al.* 1984) K_e was not given and the entrained mass flow rate was calculated from the value of the entrainment coefficient defined as

$$K_{e,gas} = \frac{\dot{m}_g + \dot{m}_o}{\dot{m}_o} \frac{D}{z} \left(\frac{\rho_o}{\rho_g}\right)^{1/2}$$

(whose values were reported in the paper) which is the usual definition of the entrainment coefficient in steady gaseous jets.

Tables 2 and 3 report the data as deduced from figures and tables of the cited references.

Figure 2(*a–d*) shows the results of the experiments. For all the experiments the dependence of $\Psi = \dot{m}_g/(\sqrt{y}\dot{m}_o)$ on y can be considered linear with acceptable

$\zeta-\zeta_o$	$K_{e,gas}$ (1)	$\zeta-\zeta_o$	m_e/m_o (2)	m_e/m_o (3)
31.25	0.348	79.2	0.220	0.221
62.5	0.278	158.4	0.309	0.364
93.75	0.261	239.6	0.474	0.618
125	0.283	320.8	0.673	1.015
156.25	0.278	406.1	0.970	1.390
187.5	0.273	487.3	1.191	1.809
218.75	0.267	566.5	1.379	2.316
250	0.267	649.8	1.732	2.702

TABLE 2. Entrainment coefficient (gas jet definition) from Ha *et al.* (1984) and non-dimensional entrained mass flow rate from Hosoya & Obokata (1992). Numbers in parenthesis refer to the experiments reported in table 1.

$\zeta-\zeta_o$	K_e ($\times10^{-2}$) (4)	K_e ($\times10^{-2}$) (5)	$\zeta-\zeta_o$	K_e (6)	K_e (7)	K_e (8)
1.04	0.844		10	0.067	0.0685	0.0563
3.07	1.19		30	0.0815	0.0772	0.0612
6.05	1.23		50	0.0863	0.0851	0.0619
12.37	1.28		70	0.091	0.0945	0.0661
24.83	1.46		90	0.102	0.1085	0.0688
51.79	1.795		110	0.109	0.113	0.0714
100	2.93		130	0.117	0.123	0.072
156.1	4.04		150	0.1216	0.147	0.0761
1.04		0.981	170	0.130	0.146	0.0833
2.53		1.06	190	0.137	0.15	0.0838
5.18		1.141	210	0.145	0.151	0.0839
10.20		1.33				
20.86		1.73				
31.32		1.86				
41.06		1.66				

TABLE 3. Entrainment coefficient from Ruff *et al.* (1988) and from Cossali *et al.* (1996). Numbers in parenthesis refer to the experiments reported in table 1.

accuracy except, for some experiments, in a region very close to the nozzle (see the next section for a discussion). From the linear fitting the constants γ and ζ_o were deduced and they are reported in table 1.

Under the hypothesis that the approximate form (35) holds, the values of $H_o(D/\bar{d})^{2/3}$ can be calculated and they are reported in table 1. It is interesting to note that the constancy of $H_o(D/\bar{d})^{2/3}$ for those experiments performed with different values of density ratio (experiments 6, 7 and 8) shows that the prediction of the effect of density ratio on entrainment is correct. The scattering of the values of $H_o(D/\bar{d})^{2/3}$ may be due partially to different atomization in different experiments and to the errors introduced in estimating the unknown parameters of some experiments.

5. Effects of some approximations

Many simplifying hypotheses has been introduced above and one of the most critical is the self-similarity of gas velocity, drop velocity and drop number concentration profiles. This is the main hypothesis on which the model is based and it is certainly

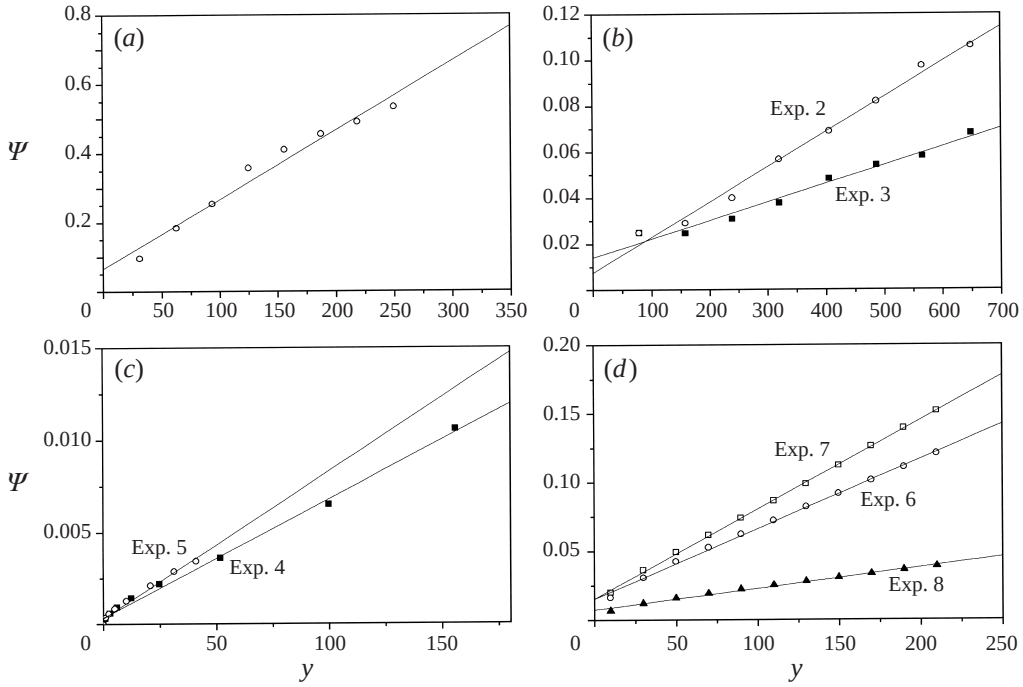

FIGURE 2. Experimental values of Ψ vs. non-dimensional nozzle distance y: (*a*) experiment 1 (Ha *et al.* 1984); (*b*) experiments 2 and 3 (Hosoya & Obokata 1992); (*c*) experiments 4 and 5 (Ruff *et al.* 1988); (*d*) experiments 6, 7 and 8 (Cossali *et al.* 1996).

acceptable for large distances from the nozzle (although complete and reliable experimental evidence does not exist at the present). But it may become questionable in the near field. Relaxation of this hypothesis will introduce a dependence on z of all the quantities M, Q, B, C, R (defined by equations (8), (9), (15), (17) and (24)), at least close enough to the nozzle, and any prediction of entrainment would require knowledge of such a dependence. The fact that the model is capable of predicting correctly the dependence of the entrained mass flow rate on z in the near field suggests that the effect of the simplification may be relevant only in a relatively narrow region very close to the nozzle (where, in fact, some experimental results show a nonlinear dependence of Ψ on y).

Another quite severe assumption is the similarity of the gas and drop velocity profiles (equation (22)). Certainly such a condition holds when drop and gas are in equilibrium (i.e. far enough from the nozzle) whereas close to the nozzle differences should be expected. It is interesting to observe that the results obtained in § 2 still hold if the difference between the shape of the gas and drop velocity profiles is small.

Let us introduce the function $\beta(\xi)$ defined as

$$\theta(\xi) = f(\xi) + \beta(\xi); \tag{37}$$

then

$$\frac{W(\xi)}{U(\xi)} f(\xi) - \theta(\xi) = G(\Phi, \varepsilon) f(\xi) - \beta(\xi)$$

and under the condition that $\beta \ll |G|f$ one can set (remembering that $-1 < G < 0$)

$$\left|\frac{W(\xi)}{U(\xi)}f(\xi)-\theta(\xi)\right|^{2/3} = |G(\Phi,\varepsilon)f(\xi)-\beta(\xi)|^{2/3} = ||G(\Phi,\varepsilon)|f(\xi)+\beta(\xi)|^{2/3}$$

$$= |G(\Phi,\varepsilon)|^{2/3}f(\xi)^{2/3}\left|1+\frac{\beta(\xi)}{|G(\xi,\varepsilon)|f(\xi)}\right|^{2/3}$$

$$\simeq |G(\Phi,\varepsilon)|^{2/3}f(\xi)^{2/3}\left(1+\frac{2}{3}\frac{\beta(\xi)}{|G(\Phi,\varepsilon)|f(\xi)}\right).$$

After introduction of the constants

$$B_f = \int_0^\infty f(\xi)\varphi(\xi)\xi\,\mathrm{d}\xi, \quad B_\beta = \int_0^\infty \beta(\xi)\varphi(\xi)\xi\,\mathrm{d}\xi,$$

$$R_\beta = \int_0^\infty \beta(\xi)f^{2/3}(\xi)\varphi(\xi)\xi\,\mathrm{d}\xi, \quad R_{2\beta} = \int_0^\infty \beta^2(\xi)f^{-1/3}(\xi)\varphi(\xi)\xi\,\mathrm{d}\xi,$$

(then $B = B_f + B_\beta$) equation (30) becomes

$$\frac{\mathrm{d}\Phi^2}{\mathrm{d}\eta} = -G(\Phi,\varepsilon)[1+\sigma|G(\Phi,\varepsilon)(1-\Phi^2)|^{2/3}]$$

$$-\sigma|1-\Phi^2|^{2/3}\left\{|G(\Phi,\varepsilon)|^{2/3}\frac{R_\beta}{3R}+|G(\Phi,\varepsilon)|^{-1/3}\frac{2R_{2\beta}}{3R}\right\}+\frac{B_\beta}{B}. \tag{38}$$

Now the limiting solution for $\zeta \to \zeta_o$ becomes

$$\frac{\mathrm{d}\Phi^2}{\mathrm{d}\eta} = 1+\sigma|G(\Phi,\varepsilon)(1-\Phi^2)|^{2/3}\left(1-\frac{R_\beta+2R_{2\beta}}{R}\right)$$

$$= 1+\sigma'|G(\Phi,\varepsilon)(1-\Phi^2)|^{2/3},$$

with: $\sigma' = \sigma(1-(R_\beta+2R_{2\beta})/R)$, showing that under the weaker assumption that the gas and drop velocity profiles are not identical (but not very dissimilar i.e. $\beta \ll f$) the limiting solutions (32) and (33) still hold (with σ substituted by σ').

The relation used to evaluate the drag on a liquid drop (equation (19)) holds for $Re < 1000$, whereas for $Re > 1000$ the following relation should be used (see, among others, Lee & Reitz 1999):

$$f_D = 3\pi\mu d''(v_g-u_d)\frac{Re}{24}\,0.424,$$

which means that the model underestimates the drag for $Re > 1000$. The region where $Re > 1000$ is close to the nozzle (where drop velocities are high and gas velocity is low) and for subsonic sprays is expected to be relatively short. In this region the momentum source, and thus entrainment, is underestimated.

Also, the effect of drop oscillation and distortion (caused by the aerodynamic forces) on drag is neglected, an assumption that is expected to underestimate the drop drag (see Hwang, Liu & Reitz 1996; Liu & Reitz 1993; and again Lee & Reitz 1999 for a discussion) although again in a region where drop–gas relative velocity is high, i.e. very close to the nozzle.

In deriving equation (30) constant values of the diameters d, d' and d'' were assumed. The mean drop diameter over a section is expected to vary with distance from the nozzle (and also when coalescence and break-up are neglected), as the different effect

of drag on drops of different diameter may cause size stratification along the spray. Again, only partial data on drop size inside the spray cone are available (due to the difficulty in measuring drop diameter in dense full cone sprays), but the agreement between prediction and experiments shown in the previous section suggests that the mean diameter may depend on z only in a quite narrow region close to the nozzle.

6. Conclusions

The model developed here allows the prediction of some important features of the gas entrainment mechanism in steady full cone sprays:

(*a*) The entrained mass flow rate depends on the distance from the nozzle in a way quite different from that found in steady gaseous jets. In the near field the entrained mass flow rate follows a 3/2-power law, which leads to a 1/2-power law of the normalized entrainment rate, whereas in the far field the linear dependence of the entrained mass flow rate on nozzle distance (as in gas jets) is recovered.

(*b*) Comparison with available experimental data seems to confirm this dependence on nozzle distance in the near field with acceptable accuracy.

(*c*) Two new non-dimensional parameters are found to characterize the entrainment process, namely the non-dimensional mean drop diameter $\bar{d}/D$ and the non-dimensional group $\mu D/\dot{m}_o$. This explains why the experimental results reported in the form of jet entrainment coefficient or normalized entrainment rate (which do not contain such parameters) under different conditions do not show consistency.

Appendix

Equation (28) was obtained as follows. From equation (6) and equation (21)

$$W(z) = \frac{\Lambda(z)\dot{m}_o}{2\pi z D \rho_g Q}; \tag{A 1}$$

from equation (18), (16), (12) and (14)

$$\frac{J_s^g(z_o, z)}{J_o} = 1 - \frac{J^l(z)}{J_o} = 1 - U(z)\frac{C}{B}\frac{\rho_o \pi D^2}{4\dot{m}_o C_M}\left(\frac{d'(z)}{d(z)}\right)^3; \tag{A 2}$$

from equation (21)

$$U(z) = (F - \Lambda(z)^2)\frac{MB}{Q^2 C}\left(\frac{d(z)}{d'(z)}\right)^3\left(\frac{\dot{m}_o}{2\pi\rho_g D^2}\right), \tag{A 3}$$

where

$$F = \frac{\rho_g}{\rho_o}\frac{8Q^2 C_M}{M}.$$

It is then possible to calculate

$$\frac{W(z)}{U(z)} = \frac{\Lambda(z)}{z(F - \Lambda(z)^2)}\frac{QC}{MB}\left(\frac{d'(z)}{d(z)}\right)^3 \tag{A 4}$$

and

$$\left(\frac{\rho_g d''(z) U(z)}{\mu}\right) = \frac{MB}{2\pi Q^2 C}(F - \Lambda(z)^2)\left(\frac{d(z)}{d'(z)}\right)^3\frac{d''(z)}{D}\frac{\dot{m}_o}{\mu D}. \tag{A 5}$$

By using the function $G(\zeta)$ (equation (27)), equation (26) becomes:

$$\frac{\mathrm{d}\Lambda^2(\zeta)}{\mathrm{d}\zeta} = -18\left(\frac{\mu D}{\dot{m}_o}\right)\left(\frac{\rho_g}{\rho_o}\right)\left(\frac{2\pi Q^2}{M}\right)\left(\frac{D^2 d''(\zeta)}{d(\zeta)^3}\right) G(\zeta) \times \left\{1 + \frac{1}{6}\left[\frac{BM}{2\pi C Q^2}(F - \Lambda(\zeta)^2)\frac{d''(\zeta)}{D}\left(\frac{d(\zeta)}{d'(\zeta)}\right)^3 \frac{\dot{m}_o}{\mu D}\right]^{2/3} \frac{R}{B}|G(\zeta)|^{2/3}\right\}.$$

REFERENCES

Cossali, G. E., Brunello, G. & Coghe, A. 1991 LDV Characterization of air entrainment in transient diesel sprays. *SAE Paper* 910178.

Cossali, G. E., Coghe, A., Gerla, A. & Brunello, G. 1996 Effect of gas density and temperature on air entrainment in a transient diesel spray. *SAE Paper* 960862.

Ha, J., Norisama, I., Sato, G. T., Hayashi, A. & Tanabe, H. 1984 Experimental investigation of the entrainnment into diesel spray. *SAE Paper*. 841078.

Hill, B. J. 1972 Measurement of local entrainment rate in the initial region of axisymmetric turbulent air jets. *J. Fluid Mech.* **51**, 773–779.

Hosoya, H. & Obokata, T. 1992 LDA measurements of spray flow from a single hole diesel type nozzle under steady conditions. In *Proc. 6th Intl Symp. on Applications of Laser Technology to Fluid Mechanics*, 37.5. Inst. Superior Tecnico, Lisbon-Portugal.

Hwang, S. S., Liu, Z. & Reitz, R. D. 1996 Breakup mechanism and drag coefficients of high speed vaporizing liquid drops. *Atomization and Sprays* **6**, 353–376.

Lee, C. H. & Reitz, R. D. 1999 Modelling the effect of gas density on the drop trajectory and breakup size of high speeed liquid drops. *Atomization and Sprays* **9**, 497–517.

Liu, Z. & Reitz, R. D. 1993 Effect of drop drag and breakup on fuel spray. *Atomization and Sprays* **3**, 55–75.

O'Rourke, P. J. & Bracco, F. V. 1980 Modelling of drop interaction in thick sprays and a comparison with experiments. *Proc. Inst. Mech. Engrs* **8**, 101–111.

Reitz, R. D. 1987 Modelling atomization processes in high-pressure vaporization sprays. *Atomization and Spray Techn.* **3**, 309–337.

Reitz, R. D. & Diwakar, R. 1987 Structure of high-pressure fuel sprays. *SAE Paper* 870598.

Ricou, F. P. & Spalding, D. B. 1960 Measurements of entrainment by axisymmetrical turbulent jets. *J. Fluid Mech.* **11**, 21–32.

Ruff, G. A., Sagar, A. D. & Faeth, G. M. 1988 Structure and mixing properties of pressure-atomized sprays. *AIAA Paper* 88-0237.

Schlichting, H. 1968 *Boundary Layer Theory*. Mc-Graw Hill.

Watkins, A. P., Gosman, A. D. & Tabrizi, B. S. 1986 Calculation of three dimensional spray motion in engines. *SAE Paper* 860468.

Wu, K.-J., Santavicca, D. A., Bracco, F. V. & Coghe, A. 1984 LDV measurements of drop velocity in diesel sprays. *AIAA J.* **22**, 1263–1270.

Wygnanski, I. & Fiedler, H. 1969 Some measurements in the self-preserving jet. *J. Fluid Mech.* **38**, 577–611.